J. Fac. Pharm. Ankara / Ankara Ecz. Fak. Derg., 49(1): 21-41, 2025
Doi: 10.33483/jfpau.1512113

ORIGINAL ARTICLE / ÖZGÜN MAKALE

MUSHROOM DERIVED COMPOUNDS UNVEILED NARINGIN AS A POTENTIAL MULTI-TARGETED ANTI-BREAST CANCER COMPOUND - AN *IN-SILICO* APPROACH

MANTAR TÜRETİLMİŞ BİLEŞİKLER, NARİNGİN'İN POTANSİYEL ÇOK HEDEFLİ MEME KANSERİ KARŞITI BİR BİLEŞİK OLDUĞUNU ORTAYA ÇIKARDI - BİR İN-SİLİCO *YAKLAŞIMI*

Ravichandran VEERASAMY[1,2]*, Raghuraman SEENIVASAN[3], Harish RAJAK[4], Parasuraman PAVADAI[5], Prabha THANGAVELU[6]

[1]AIMST University, Faculty of Pharmacy, 08100, Semeling, Malaysia
[2]Saveetha University, Saveetha Dental College and Hospitals, Saveetha Institute of Medical and Technical Sciences, Chennai, Tamil Nadu, India
[3]Shri Venkateshwara College of Pharmacy, Department of Pharmaceutical Chemistry, Ariyur, Pondicherry, India
[4]Guru Ghasidas University, Department of Pharmacy, Bilaspur, India
[5]M.S. Ramaiah University of Applied Sciences, Faculty of Pharmacy, Department of Pharmaceutical Chemistry, Mathikere, Bangaluru, Karnataka, India
[6]Nandha College of Pharmacy, Department of Pharmaceutical Chemistry, Erode, India

ABSTRACT

Objective: *The study aimed to evaluate the multiple target effect of phytochemicals of mushroom against breast cancer using molecular docking and dynamics approach.*
Material and Method: *In this study, the binding affinity of forty mushroom phytochemicals with various breast cancer proteins such as epidermal growth factor receptor (EGFR), human epidermal growth factor receptor 2 (HER2), topoisomerase IIα and topoisomerase IIβ were investigated by docking study using the PyRx tool. The selected receptors are highly cancer influencing and they were selected based on literature. Further molecular dynamics studies were also carried out to confirm the stability and conformation of the naringin-protein complex. In-silico ADMET studies were also carried out to confirm the pharmacokinetic properties and toxicity of the mushroom phytochemicals.*
Result and Discussion: *From the results obtained, colossolactone G, antcin-A, and formipinioside had higher affinity to EGFR than normal neratinib. Furthermore, fomitoside K, naringin and antcin-A were found to have higher binding affinity than neratinib with HER2. Besides, ergone, naringin, and ergosterol showed higher binding affinity than doxorubicin during interactions with topoisomerase IIα. On the other hand, antrocin, ergosterol peroxide and naringin demonstrated higher binding affinity against topoisomerase IIβ than doxorubicin. Further molecular dynamics studies were also carried out to confirm the stability and conformation of the naringin-protein complex which revealed the best binding score against all the four tested enzymes. Overall, this study suggests naringin as the best ligand and may have great potential in breast cancer protein inhibitors development. To demonstrate their therapeutic promise against breast cancer, more in vitro and in vivo research might be required.*
Keywords: *Breast cancer, molecular docking, molecular dynamics, mushroom, naringin*

* **Corresponding Author / Sorumlu Yazar:** Ravichandran Veerasamy
e-mail / e-posta: phravi75@rediffmail.com, **Phone / Tel.:** +044298000/1278

Submitted / Gönderilme : 09.07.2024
Accepted / Kabul : 30.09.2024
Published / Yayınlanma : 20.01.2025

ÖZ

Amaç: *Çalışma, mantar fitokimyasallarının meme kanserine karşı çoklu hedef etkisini moleküler yerleştirme ve dinamik yaklaşımı kullanarak değerlendirmeyi amaçladı.*

Gereç ve Yöntem: *Bu çalışmada PyRx aracını kullanarak kırk mantar fitokimyasalının epidermal büyüme faktörü reseptörü (EGFR), insan epidermal büyüme faktörü reseptörü 2 (HER2), topoizomeraz IIα ve topoizomeraz IIβ gibi çeşitli meme kanseri proteinlerine bağlanma afinitesi docking çalışmasıyla araştırıldı. Seçilen reseptörler yüksek oranda kansere etki etmektedir ve literatüre dayanılarak seçilmiştir. Naringin-protein kompleksinin stabilitesini ve konformasyonunu doğrulamak için daha ileri moleküler dinamik çalışmalar da yapıldı. Mantar fitokimyasallarının farmakokinetik özelliklerini ve toksisitesini doğrulamak için in-silico ADMET çalışmaları da yapıldı.*

Sonuç ve Tartışma: *Elde edilen sonuçlara göre kolossolakton G, antcin-A ve formipiniosidin EGFR'ye afinitesi normal neratinib'e göre daha yüksekti. Ayrıca fomitosid K, naringin ve antcin-A'nın HER2 ile neratinibden daha yüksek bağlanma afinitesine sahip olduğu bulunmuştur. Ayrıca ergon, naringin ve ergosterol, topoizomeraz IIα ile etkileşimler sırasında doksorubisinden daha yüksek bağlanma afinitesi göstermiştir. Öte yandan antrosin, ergosterol peroksit ve naringin topoizomeraz IIβ'ya karşı doksorubisinden daha yüksek bağlanma afinitesi göstermiştir. Test edilen dört enzimin tümüne karşı en iyi bağlanma skorunu ortaya koyan naringin-protein kompleksinin stabilitesini ve konformasyonunu doğrulamak için daha ileri moleküler dinamik çalışmalar da yapıldı. Genel olarak bu çalışma, naringinin en iyi ligand olduğunu ve meme kanseri protein inhibitörlerinin geliştirilmesinde büyük potansiyele sahip olabileceğini öne sürüyor. Meme kanserine karşı tedavi vaatlerini göstermek için daha fazla in vitro ve in vivo araştırmaya ihtiyaç duyulabilir.*

Anahtar Kelimeler: *Mantar, meme kanseri, moleküler dinamik, moleküler kenetlenme, naringin*

INTRODUCTION

Female breast cancer surpassed lung cancer as the major cause of global cancer incidence. Breast cancer (BC) accounts for 11.7% of all cancer cases and contributes to 685.000 deaths worldwide, making it the fifth highest cause of cancer mortality. Although geo-graphical variances occur between countries, BC remains the top cause of death in women aged 20 to 50 years [1]. Beside BC is the most common cancer in women around the world, and it is curable in 70-80% of patients with early-stage, non-metastatic cancer. Although the prevalence of BC is higher in developing countries, the rates of BC are escalating in almost every nation around the globe [2].

BC is widely recognized as a highly heterogeneous cancer type [3], encompassing distinct phenotypic and morphological profiles, resulting in highly distinctive clinical behaviors [4]. Clinically, BC is categorized into three basic types based on histological classification. They are hormone receptor positive, HER2 positive (HER2+), and triple negative BCs. Among the crucial hallmarks of cancer, angiogenesis plays a significant role particularly in BC. Vascular endothelial growth factor (VEGF) holds the title of the most potent stimulator of angiogenesis [5]. Topoisomerase II exists in mammalian cells in two closely related isoforms: topoisomerase IIα (170 kDa form) and isoforms: topoisomerase IIβ (180 kDa form). Breast cancer cells exhibit increased isoforms: topoisomerase IIα expression. So, isoforms: topoisomerase II inhibitors could exert anti-tumor effects on breast cancer [6-9].

For the past few decades, phytoconstituents of natural products have been extensively used for the treatment of cancer with high efficacy and minimal side effects [10]. Generally, traditional knowledge has led researchers to screen activity in plants, animals, and mushrooms for drug discovery from natural products. However, increasing numbers of scientists are interested in less expensive and time-consuming approaches of identifying potential compounds for specific targets, such as *in-silico* screening of previously reported substances [11-14].

Mushrooms are a valuable natural source of both food and medicine. Polysaccharides, proteins, lipids, phenols, tocopherols, alkaloids, flavonoids, carotenoids, ash, folic acid, essential oils, ascorbate enzymes, glycosides, and organic acids are some of the bio-active chemicals found in fungi which have demonstrated a wide range of pharmacological activity. Furthermore, krestin, calcaelin, hispolone, ganocidin, lectin, illudin S, hericium erinaceus polysaccharides A and B (HPA and HPB), lentinan,

schizophyllan, psilocybin, laccase, and a wide range of active compounds in mushrooms have exhibited anticancer potential [15]. Mushroom extracts and mushroom bioactive compounds have also been reported for activities, such as anticancer, antioxidative, antibacterial, antiviral, anti-inflammatory and other effects [16-20]. Besides, edible mushrooms have been used in cancer treatment, as an adjunct to conventional treatment or as a means of combating the side effects of cancer treatment. Extracts and substances isolated from fungi exhibited multiple mechanisms of anticancer activity; for example, they are reported to exert their effects by inhibiting kinases and the cell cycle or inhibiting angiogenesis and inducing reactive oxygen species, antimitotic agents, or topoisomerase inhibitor's function, ultimately stimulating apoptosis in cancer cells. Moreover, mushroom consumption reduces breast cancer risk and thus prevents ER+/PR+ tumors in breast cancer patients [17,21].

Although there are conventional cancer treatments such as surgery, radiotherapy and chemotherapy, their side effects can cause serious harm and suffering to patients. Nowadays patients give great importance to the quality of life and opt for natural products which exhibit minimal side effects as a treatment option. Mushrooms are natural resources with minimally toxic bioactive components and have various useful biological activities. Mushroom species are the most effective natural remedies against various cancers. However, 90% of mushroom species have never been studied for their antitumor effects. In addition, cancer-associated fungi studies have been performed that only involve the characterization of non-specific cytotoxic or cytostatic effects on cancer cells [11,16,22]. Therefore, compounds derived from mushrooms are of great interest for the development of anti-cancer drugs. Molecular docking studies of mushroom phytochemicals against various targets implicated in breast cancer development will determine the likelihood and mechanism of these compounds as potential breast cancer treatments.

This study aimed to study the molecular interaction between mushroom phytochemicals and breast cancer proteins through molecular docking and hypothesized that fungal phytochemicals might exert their inhibitory effect on breast cancer by interacting with breast cancer proteins. In this molecular docking study, naringin was found to be the best ligand to inhibit breast cancer proteins.

MATERIAL AND METHOD

The structure of chemical compounds derived from mushroom and proteins (Breast Cancer) were collected from online databases like PubChem and Protein Data Bank, respectively. The modeling software Chem. Office-16 (www.cambridgesoft.com/Ensemble_for_Chemistry/details/Default.aspx?fid=16), Discovery Studio Client 2021 (https://discover.3ds.com/discovery-studio-visualizer-download), Swiss Protein Data Base Viewer (https://spdbv.vital-it.ch/), PyRx (https://pyrx.sourceforge.io/), were used in the present research study.

Preparation of Phytochemicals of Mushroom

The structure of the phytochemicals of mushroom were downloaded from PubChem and checked. The selected structures were subjected for energy / geometry optimization by using MM2 force field techniques in Chem3D tool of Chem. Office 16. Then charges were added and then saved as '.sdf' file for further use.

Preparation of Protein (Breast Cancer)

The X-ray crystallographic structure of proteins of breast cancer EGFR, HER2, topoisomerase IIα and topoisomerase IIβ were downloaded from Protein Data Bank (PDB) (http://www.rcsb.org). The downloaded EGFR, HER2, topoisomerase IIα and topoisomerase IIβ are non-mutated with resolutions of 2.60 Å, 3.21 Å, 2.90 Å, and 2.55 Å, respectively. The structures of proteins were checked for any missed atoms using Swiss Protein Data Base Viewer and fixed. The information about the active site of the proteins (XYZ coordinates) were retrieved from PDB and gathered from related published articles, as well as determined by using Discover Studio Client 2021. Then water and other hetero atoms were removed from the structure of protein by using the tools available in Discovery Studio Client 2021 with default setting. Hydrogen atoms were added to the proteins and saved as in '.pdb' format.

Docking Studies

The Virtual Screening software interface PyRx (AutoDock Vina docking mechanism) was used to upload selected chemical compounds and protein structures. Before docking, the protein molecules were transformed to macromolecules. Then, using PyRx's relevant tools, both chemical compounds and protein structures were converted into '.pdbqt' format, which automatically minimized energy and incorporated charges to both micro and macromolecules. The active binding site grid box was created by utilizing the capabilities offered in PyRx. The docking was then done in PyRx with the AutoDock Vina utility. The docking or binding affinity scores with different conformers of the chemical compound were displayed by the software once the docking studies were completed. The docking output files were then downloaded as '.csv' files. The chemical compounds with the lowest energy conformers were chosen and examined for interaction with amino acids of protein utilizing Discovery Studio Client 2021. To observe the binding interactions between ligand and target, representations of the docking pose and interactions were obtained and preserved [23-25]. After docking was completed, the optimal conformer was chosen based on docking affinity and better bond interaction, and the interaction mechanism was explained.

Molecular Dynamic Simulation

MD simulations were performed for EGFR, HER2, Topoisomerase IIα and Topoisomerase IIβ separately and with naringin by using online web server WebGro (https://simlab.uams.edu/) with GROMACS to perform the calculations [26-28]. The input parameters for this study were force field GROMACS9643a, box type triclinic, water model SPC, temperature 300 K, and salt type NaCl. Pressure (1bar), number of frames per simulation (1000), and simulation time (100 ns) were employed as equilibration and MD run parameters. To create the topology of melianone, the internet server GlycoBioChem PRO-DRG2 was utilized [29]. According to the information available, the docked molecules' data were put into the PRODRG2 server to generate the zip file. The following trajectories are provided by MD simulation: root mean square deviation (RMSD), root mean square fluctuation (RMSF), radius of gyration (Rg), and hydrogen bonds (HBs).

In-Silico ADME and Toxicity Studies

SWISS ADME and ProTox-II online tools were used to estimate the ADME characteristics and toxicity of mushroom phytocompounds.

RESULT AND DISCUSSION

Forty phytochemicals from mushrooms were chosen as ligands and their interactions on the proteins involved in breast cancer were studied by molecular docking techniques in the present work. The forty phytochemicals of mushrooms were chosen from the work reported by Rangsinth et al. (2021) [30]. When these phytochemicals from mushrooms were employed for *in-silico* screening of inhibition against SARS-CoV-2, they found that all the compounds had affinity towards the main protease of SARS-CoV-2. Suwannarach et al. (2020) also reviewed the antiviral activity of phytochemicals from mushrooms [31]. As a result, we selected to screen these phytochemicals against several breast cancer targets to find a few compounds that were both anti-breast cancer and anti-SARS-CoV-2. The targeted proteins, EGFR (PDB ID: 1M17), HER2 (PDB ID: 3RCD), topoisomerase IIα (PDB ID: 4FM9) and topoisomerase IIβ (PDB ID: 4G0V) were used. The binding affinities of mushroom phytochemical compounds against breast cancer target proteins were compared with NRT and DOX.

Nuclear enzymes called DNA topoisomerases catalyze the addition of topological modifications to the DNA molecule. Type II topoisomerase, known as human topoisomerase II, has been demonstrated to be a useful target in the treatment of a variety of malignancies. Topoisomerase IIα and topoisomerase IIβ are the two isoforms of this enzyme that are present in human cells. Topoisomerase IIβ expression is uniformly distributed across all cells and serves as a biomarker for cell proliferation, but topoisomerase IIα is overexpressed in proliferating cells. As a result, topoisomerase IIα is thought to be responsible for topoisomerase II inhibitors' anticancer effects [32].

NRT was selected as a standard drug in the present study to compare with tested phytocompounds since it has been proven effective *in vitro* and *in vivo* against HER2-overexpressing or mutant cancers. The EGFR (or HER1), HER2 and HER4 tyrosine kinase activity is bound and inhibited by NRT, an irreversible tyrosine kinase inhibitor, which results in decreased phosphorylation and activation of downstream signaling pathways [33].

The frequency of hydrogen bonds forming between the ligand protein complex was related to the intensity of the inhibitors' interactions with the receptors. The outcome revealed a relationship between the hydrogen bonds, hydrophobic bonds, and electrostatic bonds present in the compounds under study and the score, which represented the binding affinity of the compounds reported as binding free energy in kcal/mol [34].

Docking

The docking studies of phytocompounds of mushroom [30], neratinib (NRT) and doxorubicin (DOX) (Table 1) were carried out against EGFR, HER2, topoisomerase IIα and topoisomerase IIβ (Figure 1) of BC. The dimensions of the grid boxes of BC proteins are shown in Table 2, and Table 1 lists the binding affinities of phytocompounds against the proteins. Amino acids of proteins interacted with NRT, DOX and phytocompounds of mushroom are given in Table 3. NRT was selected as a standard drug in the present study to compare with tested phytocompounds against EGFR and HER2, since it has been proven effective *in vitro* and *in vivo* against HER2-overexpressing or mutant cancers. DOX was selected as standard for docking against topoisomerase IIα and topoisomerase IIβ since it has been proven effective *in vitro* and *in vivo* against topoisomerase IIα and topoisomerase IIβ in cancers.

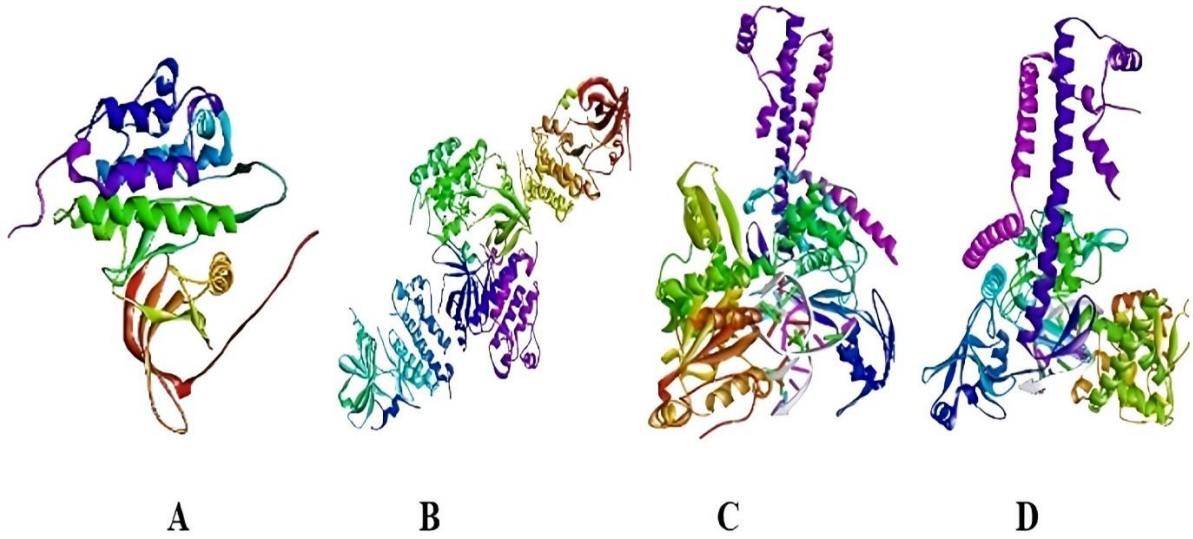

Figure 1. The PDB downloaded structure of A) EGFR (PDB ID: 1M17), B) HER2 (PDB ID: 3RCD), C) topoisomerase IIα (PDB ID: 4FM9), D) topoisomerase IIβ (PDB ID: 4G0V)

Table 1. Binding affinity among the 40 phytocompounds of mushroom and neratinib towards different breast cancer target proteins [34]

	Name of compounds	Binding affinity (kcal/mol)			
		EGFR (PDB ID: 1M17)	**HER2 (PDB ID: 3RCD)**	**Topoisomerase IIα (PDB ID: 4FM9)**	**Topoisomerase IIβ (PDB ID: 4G0V)**
1	2,3,6,23-Tetrahydroxy-urs-12-en-28-oic acid	-8.4	-8.5	-8.1	-5.3
2	Antcin-A	**-9.4**	**-9.9**	-8.8	-5.5
3	Antrocin	-6.6	-7.7	-7.9	**-6.0**
4	Antroquinonol	-6.6	-8.5	-7.5	-4.3
5	Beta-D-glucan	-7.7	-7.4	-6.9	-4.3
6	Colossolactone G	**-9.7**	**-9.7**	**-9.2**	**-5.3**
7	Cordycepin	-7.0	-7.4	-7.3	-4.7
8	Ellagic acid	-9.0	-7.9	-9.3	-5.0
9	Ergone	**-9.3**	-9.6	**-9.6**	-5.1
10	Ergosterol peroxide	**-9.1**	**-9.6**	**-9.4**	**-5.8**
11	Ergosterol	-8.8	**-9.6**	-8.7	-5.4
12	Fomitoside K	-9.1	**-9.9**	-8.4	-4.7
13	Formipinioside	**-9.2**	-8.7	-7.8	-4.6
14	Gallic acid	-5.7	-6.1	-6.4	-4.6
15	Ganoderic acid F	-9.1	-9.5	-8.7	-5.4
16	Ganoderiol A	-8.7	-8.8	-8.1	-5.1
17	Ganodermanontriol	-8.9	-9.0	-8.4	-5.0
18	Ganomycin B	-8.0	-9.4	-7.6	-4.7
19	Grifolin	-6.9	-8.4	-7.4	-4.1
20	Hispidin	-7.6	-7.7	-7.8	-5.0
21	Hispolon	-6.6	-6.7	-6.9	-4.7
22	Ibotenic acid	-5.4	-5.9	-6.3	-4.5
23	Illudin S	-6.8	-6.4	-7.8	-5.5
24	Inonotic acid A	-6.9	-7.4	-7.3	-4.7
25	L-Theanine	-5.0	-5.2	-5.6	-4.4
26	Lucialdehyde A	-8.7	-9.1	-8.3	-4.8
27	Lucialdehyde B	-8.9	-9.0	-8.8	-5.3
28	Lucialdehyde C	-8.8	-9.0	-8.2	-5.3
29	Lucidadiol	-8.5	-8.8	-8.5	-5.1
30	Lucidenic acid A	-8.3	-8.9	-8.4	-4.9
31	Lucidenic acid C	-8.6	-8.3	-7.9	-5.5
32	Lucidenic acid D	-7.8	-9.0	-8.5	-4.9
33	Lucidenic acid E	-8.1	-8.9	-8.0	-4.9
34	Lucidenic acid N	-8.1	-8.5	-8.2	-4.7
35	Lucidumol B	-8.6	-9.0	-8.2	-5.3
36	Lupeol	-8.9	-9.1	**-9.5**	-5.2
37	Naringin	**-9.1**	**-9.9**	**-9.5**	**-5.7**
38	Panepoxydone	-6.1	-6.6	-7.3	-4.7
39	Psilocybine	-6.2	-6.1	-6.9	-4.5
40	Vulpinic acid	-8.0	-8.5	-7.4	-4.7
41	NRT	-8.2	-9.4	--	--
42	DOX	--	--	-8.8	-5.1

The bolded numbers indicate the better binding affinity score for the protein. Naringin was selected to proceed with the MD simulations, as explained later. NRT – Neratinib, DOX- Doxorubicin

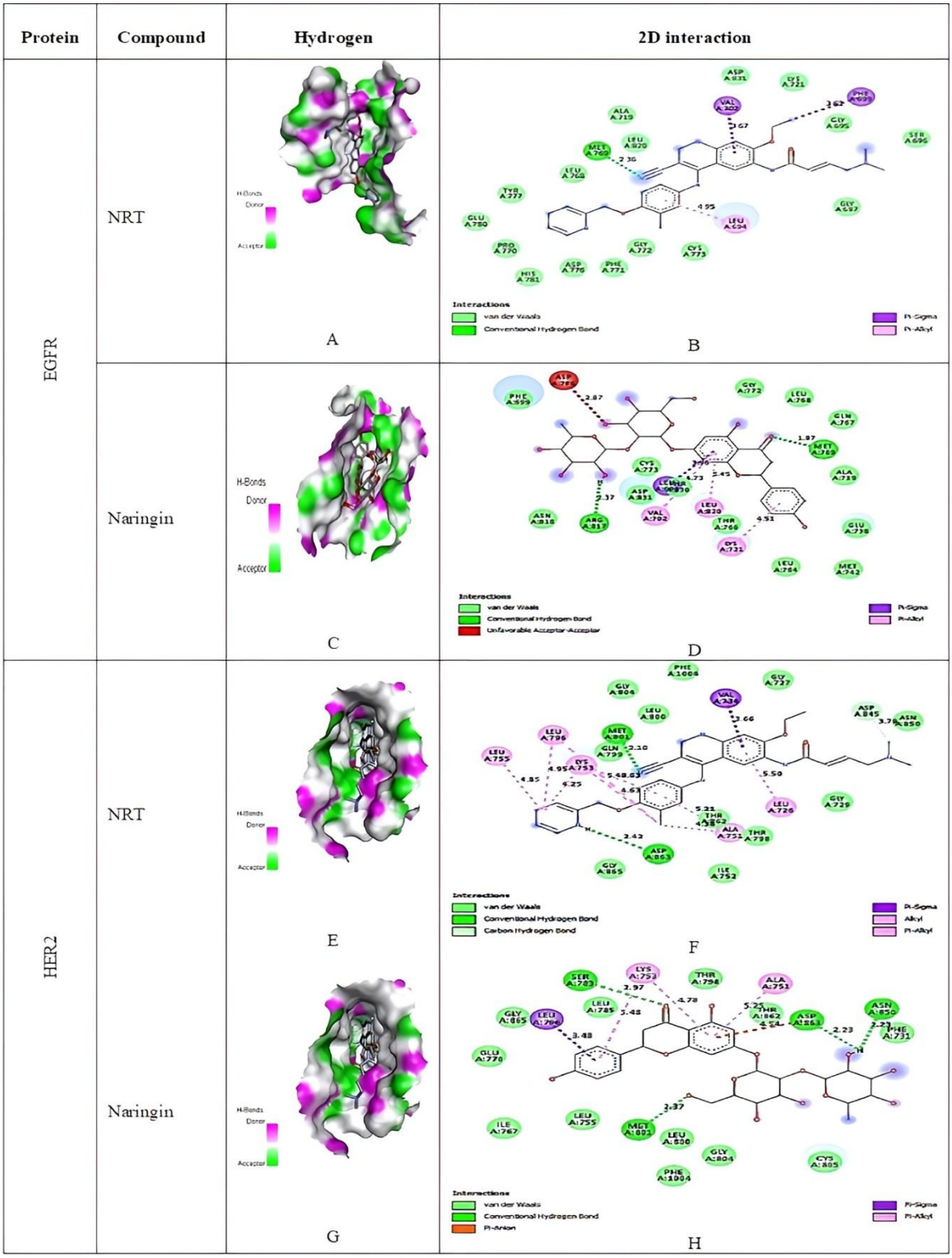

Figure 2. A) Docking pose of NRT on hydrogen bonding surface of EGFR, B) 2D interaction of NRT with EGFR, C) Docking pose of naringin on hydrogen bonding surface of EGFR, D) 2D interaction of naringin with EGFR, E) Docking pose of NRT on hydrogen bonding surface of HER2, F) 2D interaction of NRT with HER2, G) Docking pose of naringin on hydrogen bonding surface of HER2, H) 2D interaction of naringin with HER2. NRT - Neratinib

The docking pose and 2D interaction diagram of NRT and naringin with EGFR are shown in Figure 2A-2D, with HER2 are shown in Figure 2E-2H, with topoisomerase IIα are shown in Figure 3A-3D and with topoisomerase IIβ are shown in Figure 3E-3H, respectively. From the results of the current docking studies, it was found that colossolactone G, antcin-A, ergone, ergosterol peroxide, formipinioside, fomitoside K, ganoderic acid F and naringin had better finding affinity towards EGFR than NRT. Meanwhile colossolactone G, antcin-A, ergone, ergosterol peroxide, ergosterol, fomitoside K, ganoderic acid F and naringin showed better finding affinity towards HER2 than NRT. However, colossolactone G, ergone, ergosterol peroxide, lupeol and naringin exhibited better affinity towards topoisomerase IIα than NRT. Further antrocin, ergosterol peroxide and naringin shown better finding affinity towards topoisomerase IIβ than NRT.

Based on the results, the binding affinity between NRT and EGFR (PDB ID: 1M17, Figure 1A) was -8.2 kcal/mol (Table 1). The compounds with high binding affinity were colossolactone G, antcin-A, formipinioside and naringin than NRT with -9.7 kcal/mol, -9.4 kcal/mol, -9.2 kcal/mol and -9.1 kcal/mol, respectively (Table 1). All these compounds and NRT interacted with EGFR with various hydrogen bonding and hydrophobic bonding (Table 3).

NRT interacted with EGFR by forming a strong conventional hydrogen bond with Met769 as a hydrogen donor with distance of 2.36Å. It also established hydrophobic bonds such as π-sigma interaction with Val702 and Phe699 with 3.67Å and 3.62Å distance respectively, as well as π-alkyl interaction with Leu694 with distance of 4.95Å. Where Phe699 acts as π-orbitals, while Leu694 is alkyl. The amino acids that were involved in van der Waals interactions were Asp 831, Lys721, Gly695, Ser696, Gly697, Cys773, Gly772, Phe771, Asp776, His781, Pro770, Glu780, Tyr777, Leu768, Leu820 and Ala719 (Table 3, Figure 2A and B).

When colossolactone G was docked with EGFR, it formed strong conventional hydrogen bond with Thr830 with bond length 2.29Å which was stronger than two conventional hydrogen bonds formed by antcin-A with EGFR through Thr830 with distance of 2.35Å and 2.83Å. However, the conventional hydrogen bond with 2.43Å distance formed by colossolactone G with Asp831 was slightly greater than conventional hydrogen bond formed by formipinioside with Asp831 (2.42Å). Other than that, colossolactone G formed a carbon hydrogen bond with Gly772 which acts as hydrogen donor with 3.63Å distance. After docking of formipinioside to EGFR, it formed strong conventional hydrogen bond at Lys721 with distance of 2.85Å and 2.24Å. Formipinioside also formed hydrophobic bonding such as alkyl interaction with Leu694 which is an alkyl with 4.20Å and 4.59Å distance.

Meanwhile, naringin formed two conventional hydrogen bond interaction with Met769 and Arg817 of EGFR with bond length of 1.97Å and 2.37 Å (Table 1). The amino acids Leu694, Val702, Lys721, and Leu820 were hydrophobically interacted with EGFR. Amino acids Phe699, Ala719, Glu738, Met742, Leu764, Thr766, Gln767, Leu768, Gly772, Cys773, Asp831, Asn818 interacted with EGFR through van der Waals interactions (Table 3, Figure 2C and D). Even though naringin had a bit low binding affinity than colossolactone G, antcin-A, and formipinioside, it had two strong hydrogen bonds formation with EGFR compared to the earlier said three compounds. Moreover, naringin had a strong hydrogen bond with Met769 and hydrophobic interaction with Leu694 and Val702 as same as the standard drug NRT.

In addition, according to the results the binding affinity between NRT and HER2 (PDB ID: 3RCD, Figure 1B) was -9.4 kcal/mol, while the compounds of mushroom: fomitoside K, naringin and antcin-A showed better binding affinity of -9.9 kcal/mol (Table 1). Hence, these compounds were selected to compare with NRT. NRT (Figure 2E and F) and the selected compounds interacted with HER2 through various bonding interactions including hydrogen bonding and hydrophobic bonding. However, only naringin had electrostatic bonding with HER2 (Figure 2G and H).

In the case of the interaction of NRT with HER2, NRT formed strong conventional hydrogen bond with Met801 with 2.10Å distance and Asp863 with a distance of 2.42Å. It was also confirmed that a carbon hydrogen bond with Asp845 with 3.79Å distance. All these amino acids are hydrogen acceptors, except Met801 which is a hydrogen donor. Other than that, 10 hydrophobic bonds were found between the interactions of NRT and HER2 (Figure 2E and F). First, π-sigma interaction with distance of 3.66Å at Val734. The amino acids that are involved in alkyl interaction were Ala751 (4.38Å), Lys753

(4.25Å, 4.63Å), Leu796 (5.42Å, 4.95Å), Leu755 (4.85Å). Lastly, π-alkyl interactions were observed at Leu726, Ala751 and Lys753 with bond length of 5.50Å, 5.21Å and 4.63Å.

In comparison of the hydrogen bonding among NRT and selected phytochemicals, naringin formed a greater number of hydrogen bonds with HER2. Although naringin formed weaker conventional hydrogen bond with Met801 with bond length of 2.37Å than NRT (2.10 Å), it showed shorter bond length at Asp863 (2.23Å) when compared to NRT (2.42Å) and antcin-A (2.62Å, 2.17Å). The major difference is that naringin formed an electrostatic bond, π-anion, with Asp863 with bond length of 4.54Å (Figure 2G and H). However, based on the 2D interaction diagram of fomitoside K with HER2, one unfavorable bond between amino acid Asp863 and fomitoside K was observed.

Hydrophobic interactions, π-alkyl interactions, between naringin and HER2 were observed at amino acid residues, those are similar as involved in interaction with NRT, Ala751 with bond length 5.25Å and Lys753 with bond length of 4.78Å and 5.48Å (Figure 2G and H). When antcin-A docked with HER2, three alkyl interactions were observed at Val734, Ala751 and Leu852 with distance of 4.61Å, 4.65Å and 4.85Å, respectively. Alkyl interaction with amino acid Ala751 was observed in NRT. For fomitoside K, strong conventional hydrogen bonds were observed with Glu770 with bond length of 2.68Å and Gly865 with distance of 2.14Å, and both Glu770 and Gly865 act as hydrogen donor. There was also an alkyl interaction with Leu785 at bond length of 4.70Å and π-alkyl interaction with Phe864 at 5.04Å distance. Nevertheless, it does not have any similarity in interactions with HER2 as NRT and the other selected compounds.

Based on the results, the binding affinity between DOX and topoisomerase IIα (PDB ID: 4FM9, Figure 1C) was -8.8 kcal/mol, while three compounds of mushroom: ergone, naringin and ergosterol peroxide were showed better binding affinity than NRT with -9.6 kcal/mol, -9.5 kcal/mol and -9.4 kcal/mol, respectively (Table 1). Ergosterol peroxide was chosen instead of lupeol with binding affinity -9.5 kcal/mol since lupeol had lack of hydrogen bond in the docking result. The three selected compounds and DOX interacted with topoisomerase IIα through various bonding interactions including hydrogen bonding and hydrophobic bonding (Figure 3A, B, C and D). However, electrostatic interaction was observed only between naringin and topoisomerase IIα.

DOX formed three conventional hydrogen bonds with Arg727 with distances of 2.15, 2.18 and 3.03 Å as well as another conventional hydrogen bond with Arg673 (2.26Å) when docked with topoisomerase IIα (Figure 3A and B). Both Arg727 and Arg673 are acted as hydrogen donors. Glu712 as hydrogen donor formed a carbon-hydrogen bond with DOX. There were three π-cationic interactions between DOX with Arg672 (4.08 and 3.98 Å) and Lys676 (4.72 Å), and two π-anionic interactions between DOX with Glu712 (4.23 and 4.86 Å). Hydrophobic bonding such as alkyl interaction with Leu829 and Val836 with distance of 4.42Å and 4.75Å, as well as π-alkyl interaction with Arg672 (5.04Å) and Lys676 (4.54Å) were observed. In this case both amino acids act as alkyls (Figure 3A and B).

For ergone, it formed strong conventional hydrogen bond with Gln542 with Lys550 with bond length of 2.64Å and distance of 2.33Å which was shorter than the conventional hydrogen bond created between ergosterol peroxide and topoisomerase IIα. Both amino acids act as hydrogen donors. In the case of the docking of naringin with topoisomerase IIα, naringin formed strong conventional hydrogen bond with Gln544 (2.19Å), Arg672 (2.03Å), Leu685 (2.98Å) and Asp671 (2.34Å) as well as carbon hydrogen bond with Pro593 (3.24Å). Other than that, naringin also formed π-cation interaction with Arg675 (3.88Å) which was not seen in other compounds (Figure 3C and D).

According to the data obtained, the binding affinity between DOX and topoisomerase IIβ (PDB ID: 4G0V, Figure 1D) was -5.1 kcashowede the compounds of mushroom; antrocin, ergosterol peroxide and naringin were showed better binding affinity than NRT, which was -6.0 kcal/mol, -5.8 kcal/mol and -5.7 kcal/mol (Table 1). All these three compounds and DOX interacted with topoisomerase IIβ with various bonding interactions including hydrogen bonding and hydrophobic bonding, however naringin is only involved in hydrogen bonding.

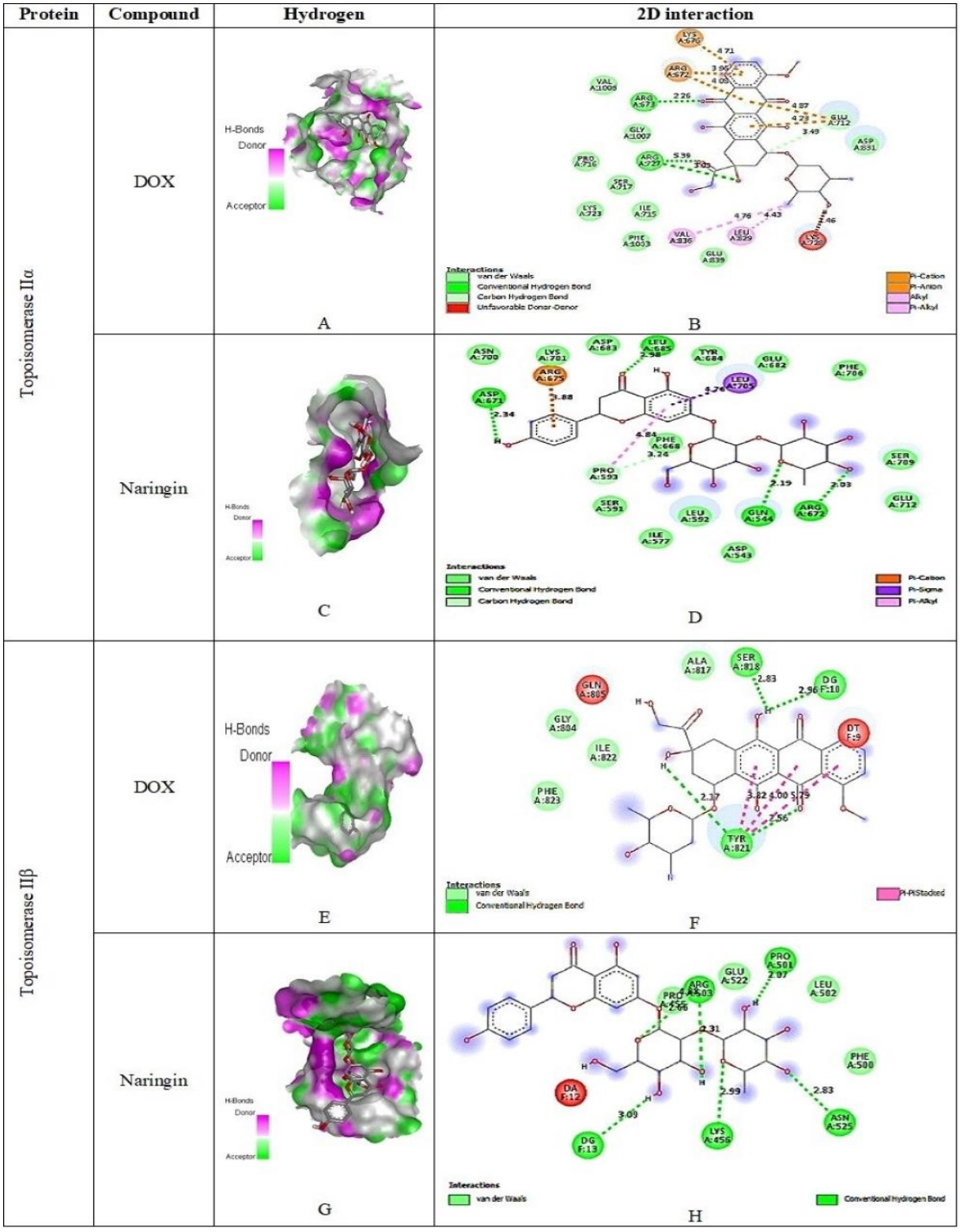

Figure 3. A) Docking pose of DOX on hydrogen bonding surface of topoisomerase IIα, B) 2D interaction of DOX with topoisomerase IIα, C) Docking pose of naringin on hydrogen bonding surface of topoisomerase IIα, D) 2D interaction of naringin with topoisomerase IIα, E) Docking pose of DOX on hydrogen bonding surface of topoisomerase IIβ, F) 2D interaction of DOX with topoisomerase IIβ, G) Docking pose of naringin on hydrogen bonding surface of topoisomerase IIβ, H) 2D interaction of naringin with topoisomerase IIβ. DOX – Doxorubicin

During the interaction of DOX with topoisomerase IIβ, DOX formed strong conventional hydrogen bond with Ser818 with bond length of 2.83 Å, Tyr821 with 2.55 and 2.17 Å distance, with Dg10 at distance 2.96Å. DOX also showed three π-π stacked bonds with Tyr821 with 3.82, 4.0, and 5.78Å distance (Figure 3E and F). For antrocin, strong conventional hydrogen bond was observed with Asn525 with 2.68Å distance and it is a hydrogen donor. Antrocin also formed π-alkyl interaction with Phe500 with bond length of 5.48Å. When ergosterol peroxide was docked with topoisomerase IIβ, it formed a strong conventional hydrogen bond with Dc11 which was a hydrogen acceptor with 3.01Å distance. Tyr821 had π-sigma interaction and π-alkyl interaction with ergosterol peroxide with distance of 3.49Å and 5.10Å respectively. On the other hand, based on the 2D interaction diagram of ergosterol peroxide with topoisomerase IIβ, three unfavorable bonds at Ser818, DNA residue Dt9 and Dg10 were observed.

Naringin owned the greatest number of hydrogen bonds with topoisomerase IIβ which were Arg503 (2.45Å, 2.66Å, 2.94Å and 2.31Å), Lys456 (2.99Å), Asn525 (2.83Å), Pro501 (2.07Å) and Dg13 (3.09Å). However, Figure 3G and H shows two conventional hydrogen bonds with Arg503 for 4.88Å and 2.66Å distance. There was one unfavorable bond with Da12 shown in 2D interaction diagram of ergosterol peroxide with topoisomerase IIβ. Antrocin and naringin did not show any similarity in interactions with topoisomerase IIβ as DOX, but ergosterol peroxide formed hydrophobic interaction with tyr821 of topoisomerase Iiβ as DOX.

Molecular Dynamic Simulation

Molecular dynamic simulation is a technique to simulate both the protein and ligand for certain time to analyze the conformation changes [35]. The trajectories acquired from MD simulations provide useful data to study the interactions between proteins and ligands. For 100 ns at 300^{o}K [36,37], MD simulations of naringin with EGFR, HER2, topoisomerase IIα and topoisomerase IIβ enzymes of breast cancer were carried out. The root means square deviation (RMSD) [38,39], root means square fluctuation (RMSF) [40], radius of gyration (Rg) [41,42] of apo and complex proteins were determined and compared.

MD simulations were performed for EGFR, HER2, topoisomerase IIα and topoisomerase IIβ. The MD results of RMSD, RMSF, radius of gyration (Rg), number of hydrogen bonds in protein and protein-naringin complex, and number of hydrogen bonds between protein and naringin against EGFR and HER2 are shown in figure 4A-4J, and against topoisomerase IIα and topoisomerase IIβ are shown in figure 5A-5J. MM-PBSA binding free energy of naringin complex of EGFR, HER2, topoisomerase IIα and topoisomerase IIβ are given in Table 2.

Figure 4A clearly indicates that the naringin-EGFR complex had a lower RMSD value than the EGFR alone, demonstrating the conformational stability of the EGFR in the presence of naringin at the active site. After 40 ns, the EGFR apo form reached equilibrium, and at 3.2 Å the EGFR reached a stable conformation. After settling and converging at 2.8 Å, the RMSD trajectory of the naringin-EGFR complex became steady after 20 ns. It has been observed that when naringin is bound, the RMSD values decrease slightly. This suggests that naringin binds tightly to EGFR and may inhibit it. Furthermore, naringin had constant fluctuations in EGFR's active pocket with an average RMSD of 4.5 Å. In RMSF studies, it was observed that a high flexibility scale for residues (725–760) of EGFR and this flexibility is due to this domain not possessing any ligands. The most residue fluctuation was observed for EGFR in the residue range 800-900 with average RMSF 1.8 Å (Figure 4B). It suggests that this domain adopted a specific conformation to accommodate naringin. EGFR and EGFR-naringin showed average Rg values of 1.93 nm and 1.99 nm, respectively (Figure 4C). Because of the binding of naringin, the complex has looser packed than EGFR, and it may be due to EGFR unfolding. Naringin did not affect the interprotein hydrogen bonding in EGFER (Figure 4D). Figure 4E depicts the results of the quantity and persistence of hydrogen bonds in the naringin-EGFR complex. Five hydrogen bonds were discovered in naringin-EGFR, and it was also supported by the results of molecular docking.

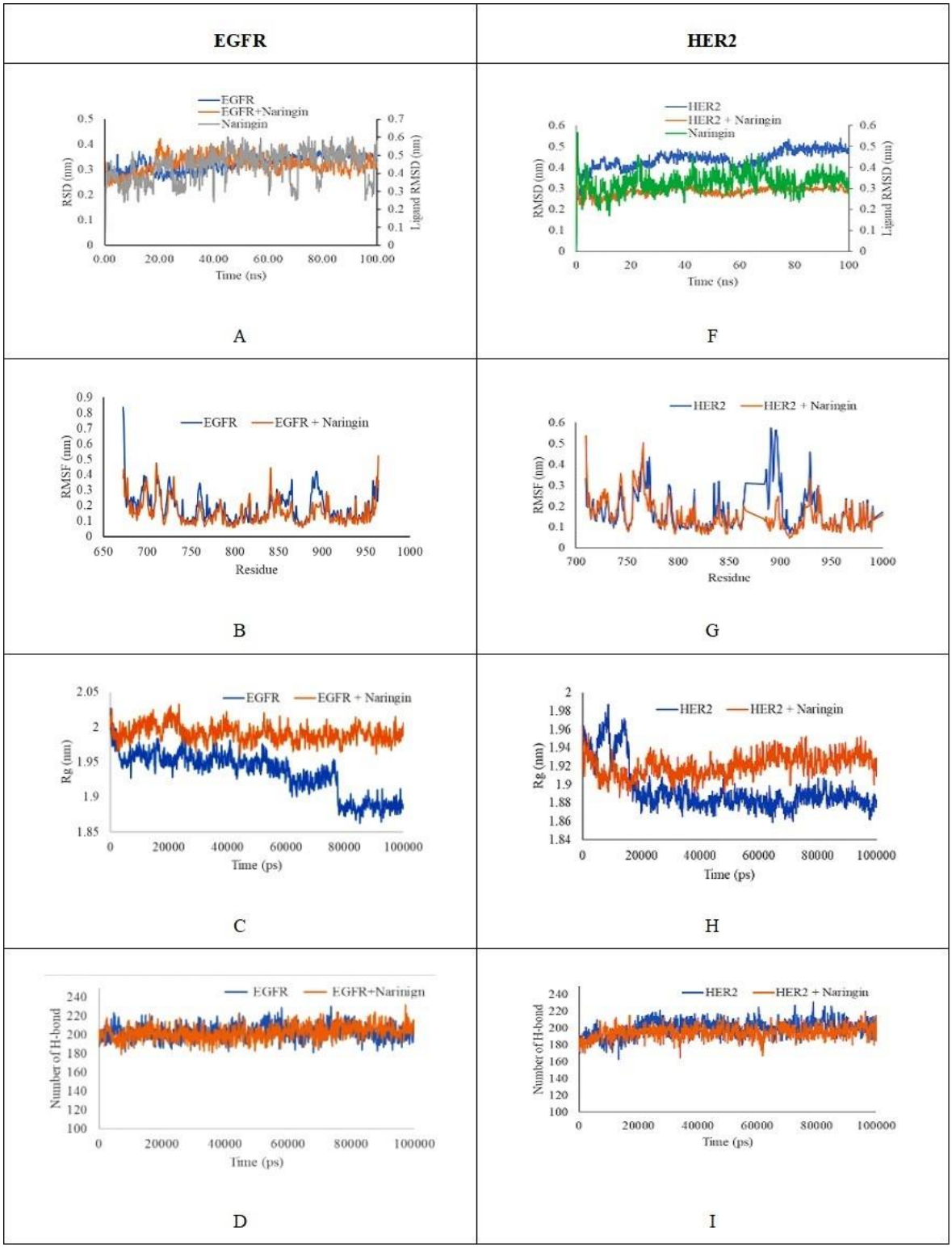

Figure 4. Molecular dynamic simulations: A) RMSD analysis of EGFR and naringin-EGFR, B) RMSF analysis of EGFR and naringin-EGFR, C) Radius of Gyration of EGFR and naringin-EGFR, D) H-Bond analysis of EGFR and naringin-EGFR, E) Lig H-Bond analysis of naringin-EGFR, F) RMSD analysis of HER2 and naringin-HER2, G) RMSF analysis of HER2 and naringin-HER2, H) Radius of Gyration of HER2 and naringin-HER2, I) H-Bond analysis of HER2 and naringin-HER2, J) Lig H-Bond analysis of naringin-HER2

The apo form of HER2 got equilibrium after 78 ns whereas and naringin complex got equilibrium after 15 ns, and the apo form of HER2 reached a stable conformation with RMSD of 5.0 Å and the complex of naringin-HER2 with RMSD of 2.9 Å that exhibited the conformational stability of the HER2 in the presence of naringin at the active site (Figure 4F). It has been observed that when naringin is bound, the RMSD values got decreased. This suggests that naringin binds tightly to HER2 and may inhibit it. Furthermore, naringin was discovered to fluctuate constantly in the active pocket of HER2 with an average RMSD of 3.2 Å. This suggests that naringin had acquired many conformations to bind tightly with HER2 and may inhibit it. In RMSF studies, it was detected that a high flexibility scale for residues (870–940) of HER2 and this flexibility may be the ligand does not possess any contact with this domain of the protein, which indicates that these sites are not stable. The most residue fluctuation was observed for EGFR in the residue range 750-860 with average RMSF 1.3 Å (Figure 4G). It confirms that this domain accommodates naringin with by possessing specific conformations. HER2 and HER2-naringin showed average Rg values of 1.88 nm and 1.93 nm, respectively (Figure 4H). Because of the binding of naringin, the complex has looser packed than HER2, and it may be due to HER2 unfolding. Both HER2 and HER2-naringin complex showed the same type of hydrogen bonding in HER2 suggested that naringin did not have any effect on the interprotein hydrogen bonding in HER2 (Figure 4I). Figure 4J il-lustrates the results of the quantity and persistence of hydrogen bonds in the nar-ingin-HER2 complex. Five hydrogen bonds were found in naringin-HER2, and it was also supported by the results of molecular docking.

Figure 5A clearly indicates that the naringin-topoisomerase IIα complex had a lower RMSD value than the topoisomerase IIα alone, demonstrating the conformational stability of the topoisomerase IIα in the presence of naringin at the active site. After 15 ns, the topoisomerase IIα apo form reached equilibrium, and at 8.0 Å the topoisomerase IIα reached a stable conformation. After settling and converging at 4.5 Å, the RMSD trajectory of the naringin-topoisomerase IIα complex became steady after 10 ns. It has been observed that when naringin is bound, the RMSD values decrease slightly. This suggests that naringin binds tightly to topoisomerase IIα and may inhibit it. But after 60 ns there was a slight increase in RMSD, indicates the binding instability of the complex. Furthermore, naringin had constant fluctuations in topoisomerase IIα active pocket with an average RMSD of 8.2 Å. In RMSF studies, it was observed that residue fluctuation was observed for topoisomerase IIα in the residue range 500-750 with average RMSF 3.3 Å (Figure 5B). It suggests that this domain adopted a specific conformation to accommodate naringin. Topoisomerase IIα and topoisomerase IIα-naringin showed average Rg values of 3.12 nm and 3.25 nm, respectively (Figure 5C). Because of the binding of naringin, the complex has looser packed than topoisomerase IIα, and it may be due to topoisomerase IIα unfolding. Naringin did not affect the interprotein hydrogen bonding in topoisomerase IIα (Figure 5D). Figure 5E depicts the results of the quantity and persistence of hydrogen bonds in naringin-topoisomerase IIα complex. Five hydrogen bonds were discovered in naringin-topoisomerase IIα, and it was also supported by the results of molecular docking.

Figure 5F clearly indicates that the naringin-topoisomerase IIβ complex had a lower RMSD value than the topoisomerase IIβ alone, demonstrating the conformational stability of the topoisomerase IIβ in the presence of naringin at the active site. After 10 ns, the topoisomerase IIβ apo form reached equilibrium, and at 8.3 Å the topoisomerase IIβ reached a stable conformation. After settling and converging at 6.2 Å, the RMSD trajectory of the naringin-topoisomerase IIβ complex became steady after 10 ns. It has been observed that when naringin is bound, the RMSD values got decreased. This suggests that naringin binds tightly to topoisomerase IIβ and may inhibit it. Furthermore, naringin had constant fluctuations in topoisomerase IIβ active pocket with an average RMSD of 9.8 Å. In RMSF studies, it was observed that residue fluctuation was observed for topoisomerase IIβ in the residue range 450-525 with average RMSF 2.5 Å (Figure 5G). It suggests that this domain adopted a specific conformation to accommodate naringin. Topoisomerase IIβ and topoisomerase IIβ-naringin showed average Rg values of 3.32 nm and 3.08 nm, respectively (Figure 5H). Because of the binding of naringin, the complex has tighter packing than topoisomerase IIβ, and it may be due to topoisomerase IIβ folding. Naringin did not affect the interprotein hydrogen bonding in topoisomerase IIβ (Figure 5I).

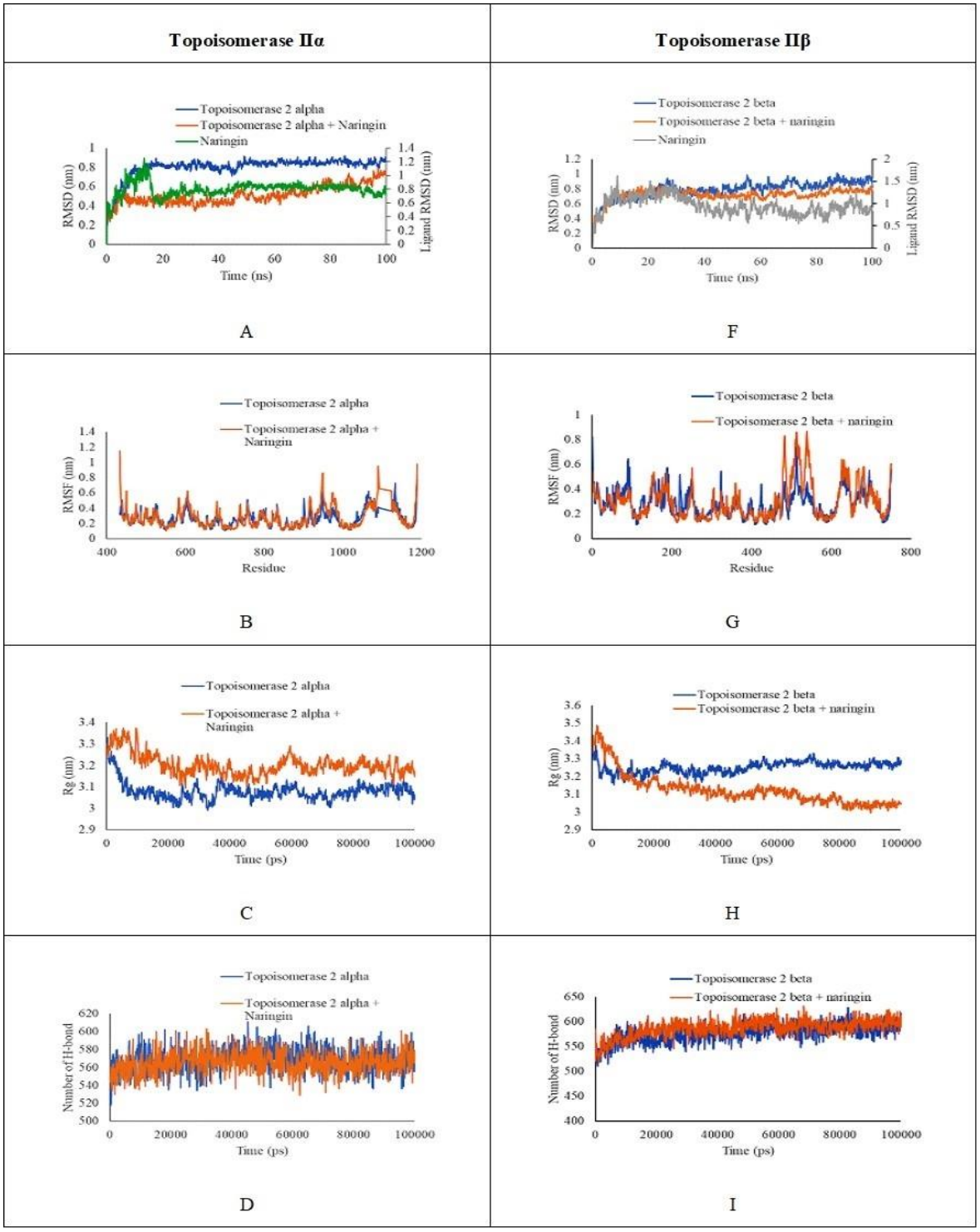

Figure 5. Molecular dynamic simulations: A) RMSD analysis of topoisomerase IIα and naringin-topoisomerase IIα, B) RMSF analysis of topoisomerase IIα and naringin- topoisomerase IIα, C) Radius of Gyration of topoisomerase IIα and naringin-topoisomerase IIα, D) H-Bond analysis of topoisomerase IIα and naringin- topoisomerase IIα, E) Lig H-Bond analysis of naringin-topoisomerase IIα, F) RMSD analysis of topoisomerase IIβ and naringin-topoisomerase IIβ, G) RMSF analysis of topoisomerase IIβ and naringin-topoisomerase IIβ, H) Radius of Gyration of topoisomerase IIβ and naringin-topoisomerase IIβ, I) H-Bond analysis of topoisomerase IIβ and naringin-topoisomerase IIβ, J) Lig H-Bond analysis of naringin-topoisomerase IIβ

The anchoring of the ligand to the protein becomes tighter as the number of hydrogen bonds increases and the length of each hydrogen bond shortens. Figure 5J depicts the results of the quantity and persistence of hydrogen bonds in naringin-topoisomerase IIβ complex. Five hydrogen bonds were discovered in naringin-topoisomerase IIβ, and it was also supported by the results of molecular docking.

Residual binding analysis is one of the key processes in structure-based drug design to identify the important residues involved in the ligand-protein binding. In residual analysis, it was noted that the hydrophobic and acidic residues in all the four used proteins made a significant impact. The results of the current investigation suggest that hydrophobic interactions between the cancer protein and naringin complexes are the primary means by which they are stabilized. The residual energy value of amino acid residues of EGFR, HER2, topoisomerase IIα and topoisomerase IIβ when these are bound with naringin are shown in Figure 1A, 1B, 1C and 1D, respectively. The key residues and their critical role in ligand binding were identified based on the contribution energy. The residual energy analysis showed that most of the residues in all four protein complexes with naringin contributed negatively. Specifically, active site residues Leu694, Val702, Ala719, Met742, Cys751, Leu764, Leu768, Pro770, Leu820, and Thr830 showed a higher contribution energy in naringin complex with EGFR however in HER2 Val734, Ala751, Met774, Leu785, Leu796, Thr798, Leu852, and Phe864 showed higher contribution energy. Active site residues Phe680, Pro681, Ile704, Leu705, Glu712, Tyr830, Glu837, and Asp1004 of topoisomerase IIα complex with naringin has shown higher contribution energy, whereas Lys1, Pro4, Phe49, Pro50, Ile75, and Ile78 are recognized as crucial residues necessary for the activity of topoisomerase IIβ.

All the examined proteins' naringin complexes (last 20 ns MD trajectories) under-went MMPBSA study to determine the van der Waals and electrostatic interactions, polar solvation, and SASA energy related with binding free energy. Table 2 comprises the binding free energy information. The strength of the binding interactions between the ligand and the target protein is measured by the ligand binding affinity, which is directly related to ligand potency. Additionally, free energy is negative for advantageous interactions. Naringin can be a possible lead for inhibiting EGFR, HER2, topoisomerase IIα and topoisomerase IIβ proteins according to MM-PBSA study, with binding free energies of -196.947, -238.847, -253.092 and -195.663 kJ mol-1, respectively. Van der Waals, electro-static, polar solvation, and SASA energy were additional energy terms that added up to yield the binding free energy.

Table 2. MM-PBSA binding free energy of naringin complex of EGFR, HER2, topoisomerase IIα and topoisomerase IIβ

Complex	van der Waal energy (kJ mol^{-1})	Electrostatic energy (kJ mol^{-1})	Polar solvation energy (kJ mol^{-1})	SASA energy (kJ mol^{-1})	Total binding energy (kJ mol^{-1})
EGFR + Naringin	-266.406 ± 18.128	-23.285 ± 8.123	115.923 ± 24.447	-23.180 ± 1.675	-196.947 ± 19.378
HER2 + Naringin	-309.133 ± 13.624	-31.821 ± 4.533	127.725 ± 12.885	-25.618 ± 1.535	-238.847 ± 18.402
Topoisomerase IIα + Naringin	-331.847 ± 11.732	-25.469 ± 12.573	130.018 ± 29.765	-25.794 ± 0.849	-253.092 ± 24.664
Topoisomerase IIβ + Naringin	-235.242 ± 23.974	-18.101 ± 9.562	78.326 ± 21.473	-20.646 ± 1.224	-195.663 ± 26.572

ADME and Toxicity Prediction of Phytocompounds Mushroom

Drug likeness, pharmacokinetic and toxicity profile are tabulated in Table 3 and 4. A drug candidate's ability to perform well in clinical trials depends on its ability to absorb, distribute, metabolize, and eliminate. Lipinski's rule of five states that an orally active medicine must have all five of the following characteristics: (i) hydrogen bond donors < 5; (ii) hydrogen bond acceptors < 10; (iii) molecular masses < 500 g/mol; and (iv) log P values less < 5 [43-45]. The pharmacokinetic characteristics of mushroom phytocompounds are displayed in Table 3. All the examined molecules,

except for a few compounds, adhere to the Lipinski rule of 5. The compound with the better binding affinity with all the four selected enzymes, naringin, however do not comply with the molecular weight, number of hydrogen bond acceptors and donors according to Lipinski rule of 5, has a medium BBB permeability, and a low clearance with score of < 5 ml/min/kg, suggesting that it may not be the best oral medication to treat breast cancer. Moreover, CYP450 2C19 substrate (non-substrate) value for naringin had a probability of 0.876; CYP450 2C19 inhibitor (non-inhibitor) had a probability of 0.986.

Table 3. Drug likeness and pharmacokinetic properties of phytocompounds of mushroom

Compounds	MW	logP	HBA	HBD	RB	TPSA	Clearance	BBB permeant	CYP2C19-inh	CYP2C19-sub
2,3,6,23-Tetrahydroxy-urs-12-en-28-oic acid	504.35	3.203	6	5	2	118.22	3.089	0.362	0.003	0.898
Antcin-A	454.31	4.581	4	1	5	71.44	15.212	0.835	0.016	0.904
Antrocin	234.16	3.667	2	0	0	26.3	10.143	0.9	0.329	0.853
Antroquinonol	390.28	6.933	4	2	11	58.92	6.455	0.078	0.467	0.887
Beta-D-glucan	504.17	-4.064	16	11	7	268.68	0.794	0.421	0.002	0.049
Colossolactone G	538.29	4.305	7	1	4	99.13	4.003	0.829	0.296	0.85
Cordycepin	251.1	-1.892	8	4	2	120.04	7.546	0.63	0.04	0.064
Ellagic acid	302.01	1.117	8	4	0	141.34	2.346	0.011	0.013	0.043
Ergone	392.31	6.157	1	0	4	17.07	2.548	0.009	0.29	0.967
Ergosterol peroxide	428.33	5.601	3	1	4	38.69	5.081	0.693	0.079	0.967
Ergosterol	396.34	5.952	1	1	4	20.23	1.97	0.861	0.051	0.974
Fomitoside K	674.44	4.461	9	4	11	142.75	2.132	0.06	0.003	0.89
Formipinioside	646.41	4.463	9	4	13	142.75	6.94	0.033	0.009	0.889
Gallic acid	170.02	0.645	5	4	1	97.99	10.108	0.099	0.026	0.039
Ganoderic acid F	512.28	2.594	7	1	6	122.65	12.787	0.937	0.025	0.907
Ganoderiol A	474.37	4.745	4	4	6	80.92	13.969	0.52	0.015	0.949
Ganodermanontriol	472.36	4.527	4	3	6	77.76	12.241	0.683	0.026	0.961
Ganomycin B	344.2	4.283	4	3	9	77.76	6.359	0.043	0.098	0.061
Grifolin	328.24	6.676	2	2	8	40.46	7.291	0.031	0.786	0.194
Hispidin	246.05	2.093	5	3	2	90.9	14.912	0.018	0.047	0.05
Hispolon	220.07	1.126	4	2	4	74.6	17.69	0.066	0.077	0.063
Ibotenic acid	158.03	-2.923	6	4	2	109.32	3.009	0.643	0.067	0.049
Illudin S	264.14	0.248	4	3	1	77.76	1.796	0.424	0.028	0.873
Inonotic acid A	270.18	1.716	4	3	5	77.76	6.567	0.786	0.014	0.272
L-Theanine	174.1	-3.109	5	4	6	92.42	5.609	0.897	0.055	0.054
Lucialdehyde A	438.35	6.138	2	1	5	37.3	6.969	0.133	0.177	0.963
Lucialdehyde B	452.33	5.136	3	0	5	51.21	7.394	0.061	0.386	0.963
Lucialdehyde C	454.34	5.311	3	1	5	54.37	9.115	0.127	0.269	0.954
Lucidadiol	456.36	5.351	3	2	5	57.53	10.902	0.384	0.121	0.949
Lucidenic acid A	458.27	2.594	6	1	4	105.58	17.353	0.651	0.009	0.942
Lucidenic acid C	476.28	2.198	7	3	4	128.97	8.818	0.662	0.003	0.82
Lucidenic acid D	514.26	2.574	8	1	6	131.88	4.62	0.739	0.024	0.879
Lucidenic acid E	516.27	2.819	8	2	6	135.04	5.833	0.741	0.015	0.824
Lucidenic acid N	460.28	2.792	6	2	4	108.74	19.628	0.575	0.005	0.909
Lucidumol B	458.38	5.321	3	3	5	60.69	10.519	0.557	0.028	0.962
Lupeol	426.39	7.291	1	1	1	20.23	17.929	0.792	0.055	0.969
Naringin	580.18	-0.493	14	8	6	225.06	1.489	0.347	0.014	0.124
Panepoxydone	210.09	2.332	4	3	3	73.22	10.311	0.037	0.043	0.58
Psilocybine	284.09	-0.701	6	2	5	82.63	3.65	0.963	0.041	0.067
Vulpinic acid	322.08	3.196	5	0	4	69.67	6.777	0.803	0.902	0.294

HBA – Hydrogen bond acceptor, HBD – Hydrogen bond donor, RB – Rotatable bond, TPSA – Total polar surface area

But like few FDA approved cancer drugs such as doxorubicin and paclitaxel with high-molecular weight (546.536Da, 800+Da), hydrogen bond donor (6.4) and acceptor (12.15), and total polar surface area (206.221), naringin which is having high-molecular weight, hydrogen bond donor and acceptors with large total polar surface area could be used as parenteral drug. Otherwise, must do some structural modification in the naringin molecule such as reduce the number of hydrogen bond acceptor count, hydrogen bond donor count and molecular weight of naringin but without any compromising on molecular interaction of naringin with cancer enzymes, to improve its ADMET properties.

Table 4. Toxicity profile of phytocompounds of mushroom

Compounds	Toxicity				
	Rat Oral Acute Toxicity	**Hepato-Toxicity**	**Carcino-Genecity**	**Respiratory Toxicity**	**Muta-Genecity**
2,3,6,23-Tetrahydroxy-urs-12-en-28-oic acid	0.359	0.198	0.037	0.522	0
Antcin-A	0.889	0.316	0.067	0.486	0
Antrocin	0.266	0.142	0.398	0.880	0
Antroquinonol	0.051	0.237	0.025	0.033	0
Beta-D-glucan	0.108	0.080	0.008	0.005	0
Colossolactone G	0.206	0.312	0.348	0.488	1
Cordycepin	0.577	0.913	0.139	0.941	0
Ellagic acid	0.450	0.144	0.314	0.067	4
Ergone	0.419	0.187	0.373	0.945	1
Ergosterol peroxide	0.986	0.584	0.064	0.975	0
Ergosterol	0.944	0.094	0.046	0.921	0
Fomitoside K	0.127	0.205	0.021	0.377	0
Formipinioside	0.106	0.526	0.075	0.100	0
Gallic acid	0.030	0.433	0.024	0.381	0
Ganoderic acid F	0.196	0.089	0.041	0.878	1
Ganoderiol A	0.044	0.605	0.041	0.967	0
Ganodermanontriol	0.068	0.605	0.345	0.973	0
Ganomycin B	0.211	0.832	0.609	0.699	0
Grifolin	0.005	0.461	0.024	0.123	0
Hispidin	0.211	0.229	0.594	0.292	0
Hispolon	0.906	0.213	0.590	0.949	1
Ibotenic acid	0.913	0.277	0.589	0.946	0
Illudin S	0.726	0.730	0.842	0.946	1
Inonotic acid A	0.055	0.211	0.032	0.072	0
L-Theanine	0.018	0.029	0.016	0.060	0
Lucialdehyde A	0.034	0.566	0.129	0.977	1
Lucialdehyde B	0.059	0.269	0.201	0.965	2
Lucialdehyde C	0.045	0.183	0.033	0.968	2
Lucidadiol	0.058	0.225	0.014	0.978	2
Lucidenic acid A	0.870	0.153	0.069	0.510	0
Lucidenic acid C	0.952	0.241	0.019	0.909	0
Lucidenic acid D	0.163	0.093	0.058	0.749	1
Lucidenic acid E	0.119	0.151	0.033	0.785	1
Lucidenic acid N	0.899	0.226	0.023	0.320	0
Lucidumol B	0.045	0.586	0.048	0.971	0
Lupeol	0.195	0.191	0.009	0.800	0
Naringin	0.245	0.103	0.795	0.033	0
Panepoxydone	0.983	0.028	0.448	0.694	0
Psilocybine	0.237	0.652	0.191	0.732	0
Vulpinic acid	0.497	0.902	0.071	0.332	1

Computational approaches for assessing and estimating the toxicity of natural bioactive chemicals are regarded as a valuable validation tool since they provide a thorough grasp of toxicogenomic. The toxicity prediction study indicates that 10 of the mushroom derived compounds are having high probability (p> 0.5) for rat oral acute toxicity, 10 compounds have high probability (p> 0.5) for hepatotoxicity, 6 compounds have high probability (p> 0.5) for carcinogenicity, 25 compounds have high probability (p> 0.5) for respiratory toxicity, and 16 compounds have high probability for mutagenicity (Table 4). However, naringin has 0.245, 0.103, 0.033 and 0 probability for rat oral acute toxicity, hepatotoxicity, carcinogenicity, and mutagenicity, respectively. Even though, naringin has 0.795 probabilities for respiratory toxicity. This can be reduced by modifying the responsible functional group in naringin without affecting the anticancer activity.

The interaction of NRT, DOX and 40 phytochemicals from mushrooms with several breast cancer enzymes such as EGFR, HER2, topoisomerase IIα and topoisomerase IIβ was investigated in this *in-silico* study. From the results, it was found that antcin-A, ergosterol peroxide and naringin were showing better binding affinity towards breast cancer proteins than the standard drug, NRT and DOX. Among all the phytocompounds of mushroom, naringin showed high binding affinity towards every breast cancer protein. Naringin exhibited optimal interactions such as more hydrogen bonding and reported the same interacted amino acids as NRT and DOX. Further the *in-silico* ADMET studies also confirmed that naringin has a low toxicity profile, but it fails to fulfill few criteria such as a greater number of hydrogen bond acceptor count, total polar surface area, molecular weight, and hydrogen bond donor count. Naringin can be ad-ministered as parental dosage form as how the FDA approved drugs paclitaxel and doxorubicin, which are also not fulfilling four out of five Lipinski criteria for oral better oral absorption. The molecular dynamic studies confirmed the stability of the molecular interaction complex of naringin with the breast cancer proteins. Hence, naringin could be suggested as the best ligand for the development of breast cancer multiple target protein inhibitors with antiviral activity. However, additional *in vitro*, preclinical, and clinical investigations are required to prove naringin's true anti-breast cancer effectiveness.

ACKNOWLEDGEMENTS

Authors are thankful to AIMST University for providing the necessary facilities to carry out this work. Author also extends thanks to Webgro online tool service for MD studies.

AUTHOR CONTRIBUTIONS

Concept: R.V.; Design: R.V., R.S.; Control: R.V., R.S.; Sources: H.R., P.P., P.T.; Materials: P.P.; Data Collection and/or Processing: H.R., P.P., P.T.; Analysis and/or Interpretation: R.V., R.S., P.P., P.T.; Literature Review: P.T.; Manuscript Writing: R.V., R.S., H.R., P.P., P.T.; Critical Reviews: R.V., R.S., H.R., P.P., P.T.; Other: -

CONFLICT OF INTEREST

The authors declare that there is no real, potential, or perceived conflict of interest for this article.

ETHICS COMMITTEE APPROVAL

The authors declare that the ethics committee approval is not required for this study.

REFERENCES

1. Sung, H., Ferlay, J., Siegel, R.L., Laversanne, M., Soerjomataram, I., Jemal, A., Bray, F. (2021). Global cancer statistics 2020: GLOBOCAN estimates of incidence and mortality worldwide for 36 cancers in 185 countries. CA: A Cancer Journal for Cinicians, 71(3), 209-249. [CrossRef]
2. Harbeck, N., Penault-Llorca, F., Cortes, J., Gnant, M., Houssami, N., Poortmans, P., Ruddy, K., Tsang, J., Cardoso, F. (2019). Breast cancer. Nature Reviews Disease Primers, 5(1), 66. [CrossRef]

3. Tomao, F., Papa, A., Zaccarelli, E., Rossi, L., Caruso, D., Minozzi, M., Vici, P., Frati, L., Tomao, S. (2015). Triple-negative breast cancer: New perspectives for targeted therapies. Onco Targets and Therapy, 177-193. [CrossRef]
4. Marusyk, A., Polyak, K. (2010). Tumor heterogeneity: Causes and consequences. Biochimica et Biophysica Acta (BBA)-Reviews on Cancer, 1805(1), 105-117. [CrossRef]
5. Wang, N., Wang, Z.Y., Mo, S.L., Loo, T.Y., Wang, D.M., Luo, H.B., Yang, D.P., Chen, Y.L., Shen, J.G., Chen, J.P. (2012). Ellagic acid, a phenolic compound, exerts anti-angiogenesis effects via VEGFR-2 signaling pathway in breast cancer. Breast Cancer Research and Treatment, 134, 943-955. [CrossRef]
6. Chen, S., Huang, L., Liu, Y., Chen, C.M., Wu, J., Shao, Z.M. (2013). The predictive and prognostic significance of pre-and post-treatment topoisomerase IIα in anthracycline-based neoadjuvant chemotherapy for local advanced breast cancer. European Journal of Surgical Oncology, 39(6), 619-626. [CrossRef]
7. Koren, R., Rath-Wolfson, L., Ram, E., Itzhac, O.B., Schachter, B., Klein, B., Gal, R., Dreznik, Z. (2004). Prognostic value of topoisomerase II in female breast cancer. Oncology Reports. 12(4), 915-919. [CrossRef]
8. Jang, J.Y., Kim, D., Kim, N.D. (2023). Recent developments in combination chemotherapy for colorectal and breast cancers with topoisomerase inhibitors. International Journal of Molecular Sciences, 24(9), 8457. [CrossRef]
9. Vanderbeeken, M.C., Aftimos, P.G., Awada, A. (2013). Topoisomerase inhibitors in metastatic breast cancer: Overview of current practice and future development. Current Breast Cancer Reports, 5(1), 31-41. [CrossRef]
10. Ekor, M. (2014). The growing use of herbal medicines: Issues relating to adverse reactions and challenges in monitoring safety. Frontiers in Pharmacology, 4, 177. [CrossRef]
11. Debnath, S., Sen, D. (2022). Mushrooms are potential foods against cancer: Identified by molecular docking and molecular dynamics simulation. Natural Product Research, 36(10), 2604-2609. [CrossRef]
12. Speck-Planche, A., Cordeiro, M.N.D.S. (2017). Fragment-based *in-silico* modeling of multi-target inhibitors against breast cancer-related proteins. Molecular Diversity, 21, 511-523. [CrossRef]
13. Sert, Y., Albayati, M.R., Şen, F., Dege, N. (2024). The DFT and *in-silico* analysis of 2,2′-((1e,1′e)-((3,3′-dimethyl-[1,1′-biphenyl]-4,4′diyl)bis(azanylylidene))bis(methanylylidene))diphenol molecule. Colloids and Surfaces A: Physicochemical and Engineering Aspects, 687, 133444. [CrossRef]
14. Mahmudov, I., Demir, Y., Sert, Y., Abdullayev, Y., Sujayev, A., Alwasel, S.H., Gulcin, I. (2022). Synthesis and inhibition profiles of *N*-benzyl-and *N*-allyl aniline derivatives against carbonic anhydrase and acetylcholinesterase-A molecular docking study. Arabian Journal of Chemistry, 15(3), 103645. [CrossRef]
15. Patel, S., Goyal, A. (2012). Recent developments in mushrooms as anti-cancer therapeutics: A review. 3 Biotech, 2, 1-5. [CrossRef]
16. Blagodatski, A., Yatsunskaya, M., Mikhailova, V., Tiasto, V., Kagansky, A., Katanaev, V.L. (2018). Medicinal mushrooms as an attractive new source of natural compounds for future cancer therapy. Oncotarget, 9(49), 29259. [CrossRef]
17. Ozturk, M., Tel-Çayan, G., Muhammad, A., Terzioğlu, P., Duru, M.E. (2015). Mushrooms: A Source Of Exciting Bioactive Compounds. In: Atta-ur-Rahman (eds). Studies in Natural Products Chemistry, (pp. 363-456). Amsterdam: Elsevier. [CrossRef]
18. Shin, A., Kim, J., Lim, S.Y., Kim, G., Sung, M.K., Lee, E.S., Ro, J. (2010). Dietary mushroom intake and the risk of breast cancer based on hormone receptor status. Nutrition and Cancer, 62(4), 476-483. [CrossRef]
19. Vamanu, E. (2018). Bioactive capacity of some Romanian wild edible mushrooms consumed mainly by local communities. Natural Product Research, 32(4), 440-443. [CrossRef]
20. Vascellari, S., Zucca, P., Perra, D., Serra, A., Piras, A., Rescigno, A. (2021). Antiproliferative and antiviral activity of methanolic extracts from Sardinian Maltese Mushroom (*Cynomorium coccineum* L.). Natural Product Research, 35(17), 2967-2971. [CrossRef]
21. Muszyńska, B., Kała, K., Sułkowska-Ziaja, K. (2017). Edible mushrooms and their *in vitro* culture as a source of anticancer compounds. In: S. Malik, (eds), Biotechnology and Production of Anti-Cancer Compounds, (pp. 231-251). Cham: Springer. [CrossRef]
22. Hao, Y.F., Jiang, J.G. (2015). Origin and evolution of China Pharmacopoeia and its implication for traditional medicines. Mini Reviews in Medicinal Chemistry, 15(7), 595-603. [CrossRef]
23. Veerasamy, R., Karunakaran, R. (2022). Molecular docking unveils the potential of andrographolide derivatives against COVID-19: An *in-silico* approach. Journal of Genetic Engineering and Biotechnology, 20(1), 1-6. [CrossRef]

24. Mun, C.S., Hui, L.Y., Sing, L.C., Karunakaran, R., Ravichandran, V. (2022). Multi-targeted molecular docking, pharmacokinetics, and drug-likeness evaluation of coumarin based compounds targeting proteins involved in development of COVID-19. Saudi Journal of Biological Sciences, 29(12), 103458. [CrossRef]
25. Hui, L.Y., Mun, C.S., Sing, L.C., Rajak, H., Karunakaran, R., Ravichandran, V. (2023). Multi-targeted molecular docking and drug-likeness evaluation of some nitrogen heterocyclic compounds targeting proteins involved in the development of COVID-19. Medicinal Chemistry, 19(3), 297-309. [CrossRef]
26. Kalimuthu, A.K., Panneerselvam, T., Pavadai, P., Pandian, S.R., Sundar, K., Murugesan, S., Ammunje, D.N., Kumar, S., Arunachalam, S., Kunjiappan, S. (2021). Pharmacoinformatics-based investigation of bioactive compounds of Rasam (South Indian recipe) against human cancer. Scientific Reports, 11(1), 21488. [CrossRef]
27. Tumskiy, R.S., Tumskaia, A.V. (2021). Multistep rational molecular design and combined docking for discovery of novel classes of inhibitors of SARS-CoV-2 main protease 3CLpro. Chemical Physics Letters, 780, 138894. [CrossRef]
28. Vishvakarma, V.K., Singh, M.B., Jain, P., Kumari, K., Singh, P. (2022). Hunting the main protease of SARS-CoV-2 by plitidepsin: Molecular docking and temperature-dependent molecular dynamics simulations. Amino Acids, 1-9. [CrossRef]
29. Schüttelkopf, A.W., Van Aalten, D.M. (2004). PRODRG: a tool for high-throughput crystallography of protein-ligand complexes. Acta Crystallographica Section D: Biological Crystallography, 60(8), 1355-63. [CrossRef]
30. Rangsinth, P., Sillapachaiyaporn, C., Nilkhet, S., Tencomnao, T., Ung, A.T., Chuchawankul, S. (2021). Mushroom-derived bioactive compounds potentially serve as the inhibitors of SARS-CoV-2 main protease: An *in-silico* approach. Journal of Traditional and Complementary Medicine, 11(2), 158-172. [CrossRef]
31. Suwannarach, N., Kumla, J., Sujarit, K., Pattananandecha, T., Saenjum, C., Lumyong, S. (2020). Natural bioactive compounds from fungi as potential candidates for protease inhibitors and immunomodulators to apply for coronaviruses. Molecules, 25(8), 1800. [CrossRef]
32. Skok, Z., Zidar, N., Kikelj, D., Ilaš, J. (2019). Dual inhibitors of human DNA topoisomerase II and other cancer-related targets. Journal of Medicinal Chemistry, 63(3), 884-904. [CrossRef]
33. Feldinger, K., Kong, A. (2015). Profile of neratinib and its potential in the treatment of breast cancer. Breast Cancer: Targets and Therapy, 147-162. [CrossRef]
34. Arthur, D.E. (2019). Molecular docking studies of some topoisomerase II inhibitors: Implications in designing of novel anticancer drugs. Radiology of Infectious Diseases, 6(2), 68-79. [CrossRef]
35. Lindorff-Larsen, K., Piana, S., Palmo, K., Maragakis, P., Klepeis, J.L., Dror, R.O., Shaw, D.E. (2010). Improved side-chain torsion potentials for the Amber ff99SB protein force field. Proteins: Structure, Function, and Bioinformatics, 78(8), 1950-1958. [CrossRef]
36. Shukla, R., Tripathi, T. (2020). Molecular Dynamics Simulation of Protein and Protein-Ligand Complexes. In: D.B. Singh, (eds), Computer-Aided Drug Design, (pp.133-161). Singapore: Springer.
37. Chen, Z., Yi, J., Zhao, H., Luan, H., Xu, M., Zhang, L., Feng, D. (2021). Strength development and deterioration mechanisms of foamed asphalt cold recycled mixture based on MD simulation. Construction and Building Materials, 269, 121324. [CrossRef]
38. Aier, I., Varadwaj, P.K., Raj, U. (2016). Structural insights into conformational stability of both wild-type and mutant EZH2 receptor. Scientific Reports, 6(1), 34984. [CrossRef]
39. Schreiner, W., Karch, R., Knapp, B., Ilieva, N. (2012). Relaxation estimation of RMSD in molecular dynamics immunosimulations. Computational and Mathematical Methods in Medicine, 2012, 173521. [CrossRef]
40. Sargsyan, K., Grauffel, C., Lim, C. (2017). How molecular size impacts RMSD applications in molecular dynamics simulations. Journal of Chemical Theory and Computation, 13(4), 1518-1524. [CrossRef]
41. Justino, G.C., Nascimento, C.P., Justino, M.C. (2021). Molecular dynamics simulations and analysis for bioinformatics undergraduate students. Biochemistry and Molecular Biology Education, 49(4), 570-582. [CrossRef]
42. Zhu, J., Lv, Y., Han, X., Xu, D., Han, W. (2017). Understanding the differences of the ligand binding/unbinding pathways between phosphorylated and non-phosphorylated ARH1 using molecular dynamics simulations. Scientific Reports, 7(1), 12439. [CrossRef]
43. Egan, W.J., Merz, K.M., Baldwin, J.J. (2000). Prediction of drug absorption using multivariate statistics. Journal of Medicinal Chemistry, 43(21), 3867-3877. [CrossRef]
44. Ghose, A.K., Viswanadhan, V.N., Wendoloski, J.J. (1999). A knowledge-based approach in designing combinatorial or medicinal chemistry libraries for drug discovery. 1. A qualitative and quantitative characterization of known drug databases. Journal of Combinatorial Chemistry, 1(1), 55-68. [CrossRef]

45. Lipinski, C.A., Lombardo, F., Dominy, B.W., Feeney, P.J. (2012). Experimental and computational approaches to estimate solubility and permeability in drug discovery and development settings. Advanced Drug Delivery Reviews, 64, 4-17. [CrossRef]